

Photon pair production and the intermediate-mass Higgs boson

Duane A. Dicus

Center for Particle Theory, University of Texas, Austin, Texas 78712

Scott S. D. Willenbrock

Physics Department, University of Wisconsin, Madison, Wisconsin 53706

(Received 9 November 1987)

We study the production of photon pairs at future hadron colliders from quark-antiquark annihilation and gluon fusion via quark loops. We show that gluon fusion is just as important as quark-antiquark annihilation for photon pairs of invariant mass less than 200 GeV, and that the gluon-fusion cross section is twice as large for a light top quark as for a heavy top quark. Photon pairs are an irreducible background to the two-photon decay mode of the Higgs boson, which is important if the Higgs boson is of intermediate mass ($m_H < 2M_W$) and $m_H < 2m_t$, i.e., if its decay to top quarks is kinematically forbidden. If that is the case, we show that the top-quark contribution to the gluon-fusion process is small and, if $m_H \approx 2m_t$, is even destructive. We also show that a judicious choice of cuts can improve the signal-to-background ratio.

I. INTRODUCTION

Future hadron colliders are being planned with an eye towards the discovery of the Higgs boson. The U.S. Superconducting Super Collider (SSC) ($\sqrt{s} = 40$ TeV) will be capable of searching for a Higgs boson as heavy as nearly 1 TeV (Ref. 1). Because of its lower energy, the CERN Large Hadron Collider (LHC) ($\sqrt{s} = 17$ TeV) will have a somewhat smaller discovery range; nevertheless, it will be able to explore masses of several hundreds of GeV (Ref. 2). These machines will take advantage of the fact that a heavy Higgs boson ($m_H > 2M_W$) decays almost exclusively to W - and Z -boson pairs, which should provide an observable signal.

If the Higgs boson is less massive than two times the W -boson mass, its decay modes make its discovery at a hadron collider much less certain. An intermediate-mass Higgs boson ($50 \text{ GeV} \lesssim m_H < 2M_W$) decays predominantly to the heaviest available fermion-antifermion pair. If $m_H > 2m_t$, the top-quark decay mode will dominate; otherwise, the Higgs boson will decay most frequently to bottom quarks. In either case there is an enormous background from ordinary QCD heavy-quark production, which masks the signal.³

The difficulty with discovering an intermediate-mass Higgs boson at a hadron collider is therefore not the rate of production, but rather the signal-to-background ratio. Indeed, one expects roughly 10^6 events/yr at the SSC, assuming a luminosity of $10^{33}/\text{cm}^2 \text{ sec}$. Now the partial decay width of the intermediate-mass Higgs boson to bottom quarks is rather small, on the order of 10 MeV, because of the small coupling involved [$(g/2)m_b/M_W$]. Therefore, if the decay to top quarks is kinematically forbidden, one may entertain the possibility of searching for the Higgs boson in one of its rare decay modes. Decays to $\tau^+\tau^-$ (Refs. 4–7), $\gamma\gamma$ (Refs. 4–9), $\Theta\gamma$ (Refs. 6 and 7) (Θ =toponium), $Z\gamma$ (Refs. 10, 6, and 7), ZZ^* , and WW^* (Refs. 11, 6, and 7) (the asterisks indicate a virtual parti-

cle) have been considered in the literature.

The two-photon decay mode^{4–9} of the intermediate-mass Higgs boson, which proceeds via W -boson and top-quark loops, is particularly promising because of the cleanliness of the final state. The branching ratio is rather small, less than 10^{-3} ; however, this still leaves about 10^3 events/yr. The important question is therefore whether the signal is observable above the continuum background.

In this paper we calculate the irreducible two-photon background in proton-proton collisions. This background is due to quark-antiquark annihilation [Fig. 1(a)] and gluon fusion [Fig. 1(b)]. The former process is well known, and we have nothing new to add to its calculation. Gluon fusion has also been considered in the literature, at future hadron colliders^{5,12} as well as at lower energies.^{13–16} However, no analysis thus far has included the contribution of the top quark to the gluon-fusion cross section. As we shall see, the top quark can potentially double the cross section, so it is important to include its contribution.

We will show that in the intermediate-mass Higgs-boson range, gluon fusion is as important as quark-antiquark annihilation for photon pair production at future hadron colliders.^{5,12} This is somewhat surprising since gluon fusion is suppressed by two powers of α_s with respect to quark-antiquark annihilation. This is largely compensated for by the large gluon luminosity at future hadron colliders. Furthermore, the gluon-fusion amplitude is larger than one might expect, as we will demonstrate.

The remainder of the paper is organized as follows. In Sec. II we calculate the hadronic cross section for photon pair production from quark-antiquark annihilation and gluon fusion, the latter for a variety of top-quark masses. In Sec. III we discuss the interference of the gluon-fusion process with the production of the Higgs boson from gluon fusion followed by two-photon decay. In Secs. IV

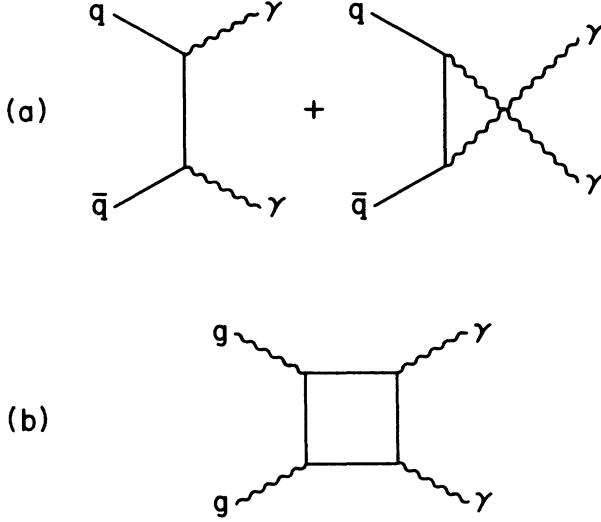


FIG. 1. Photon pair production from (a) quark-antiquark annihilation and (b) gluon fusion via a virtual quark loop. There are six box diagrams, corresponding to the $3!$ permutations of the external legs, of which three are independent.

and V we present the angular and rapidity distributions of the photon pairs. In Sec. VI we discuss photon pair production at large invariant masses, ranging from 100 GeV to 1 TeV. Finally, in Sec. VII we discuss the implications of our results for the discovery of the intermediate-mass Higgs boson via its two-photon decay mode.

II. CROSS SECTIONS

Photon pair production from gluon fusion [Fig. 1(b)] is identical, up to color factors, to the scattering of light by light. The latter process was first calculated exactly in 1951 by Karplus and Neuman using the usual Feynman techniques.¹⁷ Some years later, in 1964, it was calculated by De Tollis, using the Mandelstam representation and dispersion relations.¹⁸ This proves to be a very powerful technique for this process, and yields relatively simple helicity amplitudes. The history of this subject and its applications to a variety of processes, as well as the helicity amplitudes which we will use in this paper, are given in a review article by Constantini, De Tollis, and Pistoni.¹⁹

There are five independent helicity amplitudes, $M_{\lambda_1\lambda_2\lambda_3\lambda_4}$, which may be chosen to be M_{++++} , M_{+---} , M_{-+++} , M_{++--} , and M_{--++} . The helicities λ_1, λ_2 are for the incoming photons and λ_3, λ_4 for the outgoing photons. The remaining helicity amplitudes may be obtained from parity and permutation symmetry.

Of these five helicity amplitudes, three are related by crossing; hence it is sufficient to give just three. These are given in Eq. (93) of Ref. 19, and the various relations to obtain the other 13 helicity amplitudes are given in Eq. (92); see also Eq. (4) of this paper. Note that r, s , and t in that paper are defined in terms of the usual Mandelstam

variables s, t , and u by

$$r = \frac{1}{4} \frac{s}{m^2}, \quad s = \frac{1}{4} \frac{t}{m^2}, \quad t = \frac{1}{4} \frac{u}{m^2}, \quad (1)$$

where m is the mass of the fermion in the loop. The amplitudes are normalized such that the spin- and color-averaged differential cross section for photon pair production from gluon fusion is ($z = \cos\theta$)

$$\frac{d\sigma}{dz} = \frac{1}{64\pi} \alpha_s^2 \alpha^2 q^4 \frac{1}{s} \sum |M|^2, \quad (2)$$

where q is the charge of the fermion in the loop and the sum is over the 16 helicity amplitudes. This normalization of the amplitudes differs from the usual one by a factor of $1/(2\pi^2)$.

The helicity amplitudes of Ref. 19 are quite compact and simple to program. They are expressed in terms of certain special functions, also given in that paper. The only special function not given in closed form is the Spence (or dilogarithm) function of a complex argument.²⁰ Fortunately, a compact and rapidly converging series for this function is given in Appendix A of Ref. 21.

As a totally independent check on the helicity amplitudes of Ref. 19, we used the program FORMFACTOR²² to calculate the amplitudes numerically. We were able to confirm the validity of the helicity amplitudes to a high degree of accuracy.²³ Gauge invariance provided a very nontrivial check on the numerical computations, and assured us of the convergence of the integrations being performed.

Since the helicity amplitudes are expressed in terms of the ratios r, s , and t defined in Eq. (1), they are inadequate in the limit $m^2 \ll s, |t|, |u|$ due to roundoff errors. One must instead employ analytic expressions for the amplitudes in the $m \rightarrow 0$ limit. These are given in Ref. 13; we have checked them, and reproduce them here for later reference. Expressed in terms of the usual Mandelstam variables s, t , and u , they are

$$\begin{aligned} \text{Re}M_{++++} &= 1 + \frac{t-u}{s} \ln \left| \frac{t}{u} \right| \\ &\quad + \frac{1}{2} \frac{t^2+u^2}{s^2} \left[\ln^2 \left| \frac{t}{u} \right| + \pi^2 \theta \left(\frac{t}{u} \right) \right], \\ \text{Im}M_{++++} &= -\pi [\theta(t) - \theta(u)] \\ &\quad \times \left[\frac{t-u}{s} + \frac{t^2+u^2}{s^2} \ln \left| \frac{t}{u} \right| \right], \end{aligned} \quad (3)$$

$$M_{+++-} = -1, \quad M_{+-++} = -1.$$

The remaining 13 amplitudes may be obtained from these by using the relations

$$\begin{aligned} M_{+++-} &= M_{+-++} = M_{-+++} = M_{-++-}, \\ M_{+---}(s, t, u) &= M_{++++}(t, s, u), \\ M_{-+++}(s, t, u) &= M_{++++}(u, t, s), \end{aligned} \quad (4)$$

and parity.

The five light flavors of quarks contribute to the ampli-

tude an amount proportional to the square of their charge, the sum of which is $\frac{11}{9}$. If the top quark is light compared to the photon pair invariant mass, it contributes another $\frac{4}{9}$ to this sum. Therefore the ratio of the cross sections with and without a light top quark included is $(\frac{15}{11})^2$, i.e., roughly a factor of 2.

If the top quark is heavy compared with the photon pair invariant mass, it will make a negligible contribution to the gluon-fusion amplitude due to the decoupling of heavy particles.²⁴ In fact, we know on dimensional grounds that the amplitude decreases like $1/m_t^4$ in the

large-top-mass limit, since the only gauge-invariant operators are of dimension four (formed from the product of the field-strength tensors $F_{\mu\nu}$ of each external gauge boson) and higher. However, if the top mass is on the order of the photon pair invariant mass, we cannot draw any conclusions about its contribution to the gluon-fusion amplitude without a detailed calculation.

The photon-pair cross section in pp collisions over an invariant-mass range relevant to the intermediate-mass Higgs boson is shown in Figs. 2 (SSC) and 3 (LHC) for a variety of top-quark masses. Qualitatively, we see that gluon fusion is an equally copious source of photon pairs as quark-antiquark annihilation, regardless of the top-quark mass.

The curve for $m_t = 100$ GeV is almost identical to the curve for heavier top quarks over the invariant-mass range displayed. It therefore represents the $m_t \gg M$ limit (M is the photon pair invariant mass) in which the top quark makes no contribution to the gluon-fusion cross section. The $m_t = 25$ GeV curve represents the small m_t limit at large invariant masses; we see that it is roughly twice as large as the $m_t = 100$ GeV curve at $M = 200$ GeV, as we expect (see the discussion earlier in this section).

The dependence of the cross section on the top-quark mass when $m_t \sim M$ is remarkable. We see that there is a small dip in the cross section at $M = 2m_t$. The top quark therefore interferes destructively with the five light flavors at this invariant mass. Amazingly, this is exactly what we want phenomenologically, because $m_H \approx 2m_t$ maximizes the Higgs-boson production cross section (which also proceeds via gluon fusion) given the constraint $m_H < 2m_t$ (to eliminate the top-quark decay mode).

The spin- and color-averaged cross section for photon pair production from quark-antiquark annihilation is

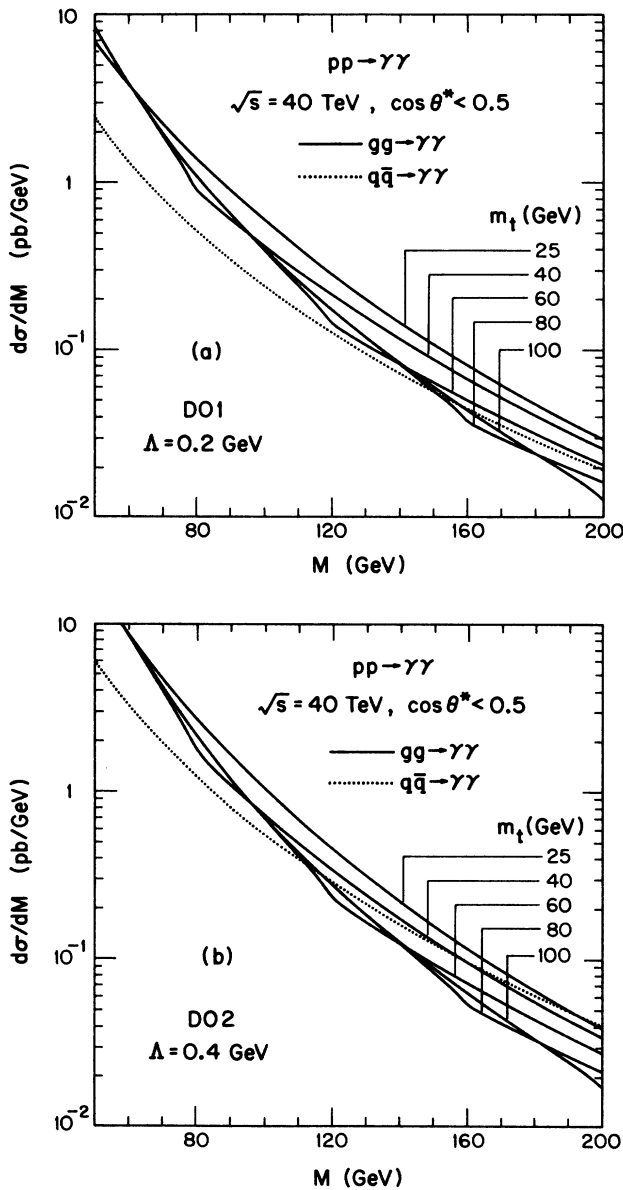


FIG. 2. Invariant-mass distribution of photon pairs produced at the SSC via quark-antiquark annihilation and gluon fusion, for a variety of top-quark masses. There is a cut on the scattering angle in the photon pair center-of-mass system, θ^* , of $\cos \theta^* < 0.5$. The distribution functions of Duke and Owens (a) set 1 and (b) set 2 were used.

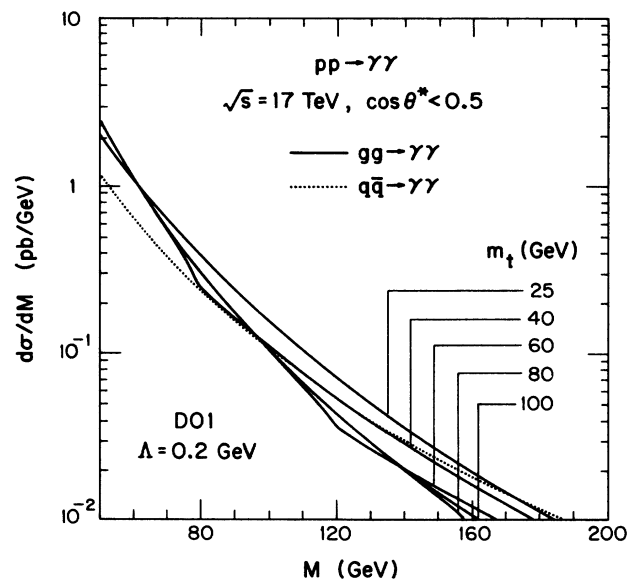


FIG. 3. Same as Fig. 2, but for the LHC. Only the results for the Duke-Owens set 1 distribution functions are given.

$$\frac{d\sigma}{dz} = \frac{\pi}{3} \alpha^2 q^4 \frac{1}{s} \left[\frac{t}{u} + \frac{u}{t} \right], \quad (5)$$

where q is the charge of the quark. This process is strongly peaked in the forward-backward direction due to the t - and u -channel poles. Since the Higgs-boson decay to two photons is isotropic, we can suppress this background by imposing a cut on the scattering angle in the photon pair center-of-mass frame θ^* . We have chosen $\cos\theta^* < 0.5$, following a recent analysis of the two-photon decay mode of the Higgs boson.⁷ Since the gluon-fusion amplitude has no t - or u -channel poles, the cross section is less strongly peaked in the forward-backward direction; however, it is enhanced there, as we will show in Sec. IV. The cut on the scattering angle is therefore important to suppress this background as well.

Since the gluon-fusion and quark-antiquark annihilation processes are initiated by different partons, we investigated the dependence of the cross sections on different sets of distribution functions. We used Duke and Owens²⁵ set 1 ($\Lambda=200$ MeV) and set 2 ($\Lambda=400$ MeV) for the comparison; the results are shown in Fig. 2. Both the gluon-fusion and the quark-antiquark annihilation cross sections are larger for set 2, the latter by roughly a factor of 2. However, the ratio of the two processes is less sensitive to the choice of distribution functions, although gluon fusion is relatively less important for set 2.

This behavior is easily understood qualitatively. Since set 2 corresponds to a larger Λ , the QCD evolution of the distribution functions to large Q^2 yields a greater density of gluons and sea quarks at small x ; hence the increased cross sections (we are using $Q^2=M^2$). The gluon-fusion cross section is also augmented by the increased value of α_s associated with a larger Λ .

Finally, let us discuss the relative size of the gluon-fusion and quark-antiquark cross sections qualitatively. (We shall neglect the top quark in the following discussion). The ratio of the two cross sections is roughly

$$\frac{\sigma(gg \rightarrow \gamma\gamma)}{\sigma(q\bar{q} \rightarrow \gamma\gamma)} \approx \frac{3}{8} \left(\frac{11}{4} \right)^2 \left[\frac{g_s^2}{2} \right]^2 \frac{\mathcal{L}_{gg} \sum |M_{gg}|^2}{\mathcal{L}_{q\bar{q}} \sum |M_{q\bar{q}}|^2}. \quad (6)$$

The first factor is from color averaging. The second is from the quark charges; the sum of the squares of the charges is $\frac{11}{9}$ for gluon fusion, while for quark-antiquark annihilation only the charge $\frac{2}{3}$ quarks are important (the cross section is proportional to q^4), which squared gives $\frac{4}{9}$. The third factor is the coupling of the gluons to the quarks; the factor of $\frac{1}{2}$ is from the trace of the color matrices in the loop: $\text{Tr} T^A T^B = \frac{1}{2} \delta^{AB}$ (Ref. 26). The fourth factor is the ratio of the gluon-gluon luminosity to the luminosity of charge $\frac{2}{3}$ quark-antiquark collisions. This is a large factor, roughly 100 in the intermediate-mass Higgs-boson mass range at SSC energies.³ The last factor is the ratio of the sum of the squared amplitudes, devoid of coupling constants. The gluon-fusion amplitudes are suppressed since they are one loop; however, they are larger than one might anticipate, as we will now discuss.²⁷

For comparison, consider the gluon-fusion and quark-antiquark amplitudes at right angles ($\theta^*=\pi/2$), i.e., $t=u=-\frac{1}{2}s$. There are four nonvanishing helicity amplitudes for quark-antiquark annihilation, each equal to 2 at right angles. There are 16 helicity amplitudes for gluon fusion. Using Eqs. (3) and (4), we find that their values at right angles are

$$\begin{aligned} M_{+ + - -} &= M_{+ + + -} = M_{+ - - +} = M_{+ - + +} \\ &= M_{- - + +} = -1, \\ M_{+ + + +} &= 1 + \frac{\pi^2}{4} = 3.46, \\ M_{+ - - +} &= M_{+ - + -} = 1 - 3 \ln 2 + \frac{5}{2} \ln^2 2 + i\pi(3 - 5 \ln 2) \\ &= 0.12 - 1.46i \end{aligned} \quad (7)$$

with the remaining eight given by parity. All of these amplitudes must be multiplied by $1/(2\pi^2)$. Therefore, most of the helicity amplitudes have a magnitude of roughly $1/(2\pi^2)$. This is surprisingly large, because loop diagrams usually have factors of $1/(8\pi^2)$ (or smaller) associated with them.²⁸ Furthermore, the amplitude $M_{+ + + +}$ is larger still, due to the π^2 term (which is reminiscent of the K factor in QCD). This helicity amplitude (and its parity conjugate) alone makes up about half of the total cross section for gluon fusion at right angles.

Putting it all together, we find that the ratio of the gluon-fusion and quark-antiquark annihilation cross section at $\theta^*=\pi/2$ is roughly

$$\frac{\sigma(gg \rightarrow \gamma\gamma)}{\sigma(q\bar{q} \rightarrow \gamma\gamma)} \approx 1, \quad (8)$$

which is what we found in our more detailed calculations.

Therefore, the reasons that gluon fusion can compete with quark-antiquark annihilation as a source of photon pairs, despite its suppression by α_s^2 , are, in order of importance, (i) the large gluon luminosity, (ii) the surprisingly large amplitudes, especially $M_{+ + + +}$, and (iii) the advantage of coherently summing all flavors of quarks in the loop [the second factor in Eq. (6)].

III. INTERFERENCE

As we discussed in the introduction, photon pair production from gluon fusion is a background to the two-photon decay mode of the intermediate-mass Higgs boson. Since the Higgs boson itself is produced from gluon fusion (via a top-quark loop),²⁹ the Higgs-boson signal has the same initial and final state as the gluon-fusion background, as is illustrated in Fig. 4. The two processes are, therefore, subject to interference.

The Higgs-boson production and decay process is only sizable near the Higgs-boson pole, where it is enhanced—after all, it is a two-loop process, compared with the gluon-fusion background, which is one-loop. Normally the interference between a resonance and a continuum process is unimportant, because on resonance the two are out of phase. Furthermore, off resonance the interference is proportional to $s - m_H^2$, which is antisym-

metric about the resonance point $s = m_H^2$. The interference therefore vanishes when integrated over an invariant-mass bin centered on the resonance.

The above argument assumes that the two processes are in phase off resonance. This would be the case if both processes were $2 \rightarrow 2$ tree diagrams, for example. However, the processes we are considering are loop diagrams, which have both real and imaginary parts. Let M_1 be the continuum gluon-fusion amplitude, and $M_2 s / (s - m_H^2 + i\Gamma_H m_H)$ be the Higgs-boson production and decay amplitude, with the Higgs resonance made explicit. The interference is then

$$2 \frac{s}{(s - m_H^2)^2 + \Gamma_H^2 m_H^2} [(\text{Re}M_1 \text{Re}M_2 + \text{Im}M_1 \text{Im}M_2)(s - m_H^2) + (\text{Re}M_1 \text{Im}M_2 - \text{Im}M_1 \text{Re}M_2)\Gamma_H m_H] . \quad (9)$$

The first term, proportional to $s - m_H^2$, integrates to zero, as we discussed. The second term does not, however. Thus, if $\text{Im}M_1$ or $\text{Im}M_2 \neq 0$ (assuming $\text{Re}M_1$ and $\text{Re}M_2 \neq 0$), then there is nontrivial interference. This effect has been studied for a related process: Higgs-boson production from gluon fusion followed by decay into heavy quarks (which has a direct QCD background).³⁰

Loop diagrams have nonzero imaginary parts only if cutting the diagram yields a kinematically allowed process. Thus the coupling of the Higgs boson to two photons has a nonzero imaginary part only if $m_H > 2M_W$ or $m_H > 2m_t$; similarly, the coupling to two gluons has an imaginary part only if $m_H > 2m_t$. However, we are interested in the scenario in which the Higgs boson cannot decay to W -boson or top-quark pairs. Therefore the amplitude for the production and two-photon decay of the Higgs boson is a real number multiplied by a Breit-Wigner resonance (i.e., M_2 is real in our example).

By the same reasoning, the top-quark loop in the gluon-fusion background process produces no imaginary part at $s = m_H^2$. The five light flavors potentially do, however. Since the Higgs production amplitude is $J = 0$, the only nonvanishing helicity amplitudes are those in which the initial helicities are equal and the final helicities are equal. Inspection of The M_{++++} and M_{++--} amplitudes for the gluon-fusion background process with massless quarks [Eq. (3)] shows that they are purely real. This is because the cut diagram, quark-antiquark production from gluon fusion, vanishes in the massless limit if the gluons have the same helicities.

Therefore, we see that both the signal and the background are purely real in the case of interest, and that the interference integrates to zero over an invariant-mass bin centered on the Higgs resonance.

IV. ANGULAR DISTRIBUTION

Since the Higgs boson is spinless, its decay to two photons is isotropic in its rest frame. Photon pair production from quark-antiquark annihilation is, on the other hand,

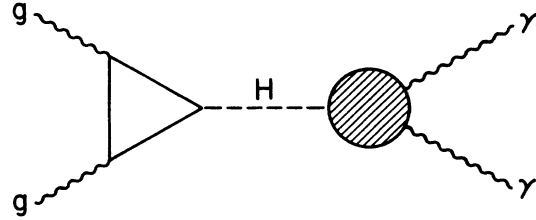


FIG. 4. Higgs-boson production from gluon fusion via a top-quark loop followed by two-photon decay. The decay proceeds via a W -boson and a top-quark loop.

strongly forward-backward peaked; the cross section is proportional to $1/t$ as $t \rightarrow 0$ due to the t -channel quark-exchange diagram in Fig. 1(a). Therefore, by restricting our attention to scattering away from the beam direction, we can enhance the signal-to-background ratio for Higgs-boson production and decay to two photons.

Since photon pair production from gluon fusion has no t - or u -channel poles, it is less singular in the forward-backward direction than quark-antiquark annihilation. Nevertheless, the cross section is enhanced at small angles. This is evidenced by the helicity amplitudes in the massless quark limit, Eqs. (3) and (4). As $t \rightarrow 0$, these amplitudes go to

$$\begin{aligned} M_{++++} &\rightarrow 1 + \frac{\pi^2}{2} - \ln \left| \frac{s}{t} \right| + \frac{1}{2} \ln^2 \left| \frac{s}{t} \right| , \\ M_{+--+} &\rightarrow 0 , \\ M_{++--} &\rightarrow 1 - \ln \left| \frac{s}{t} \right| + \frac{1}{2} \ln^2 \left| \frac{s}{t} \right| + i\pi \left[1 - \ln \left| \frac{s}{t} \right| \right] \end{aligned} \quad (10)$$

with the remaining five amplitudes (not counting the parity conjugates) equal to -1 at all angles. Thus the most singular term in the cross section is proportional to $\ln^4 |t|$ as $t \rightarrow 0$.

In Fig. 5 we show the photon-pair angular cross section as a function of the cosine of the scattering angle in the photon-pair center-of-mass frame, at an invariant mass of 120 GeV. The quark-antiquark annihilation cross section is more strongly peaked in the forward direction than that of gluon fusion, as we expect. However, both are relatively flat out to $z = 0.8$ ($\theta^* = 37^\circ$). The gluon-fusion cross section is shown for two different top-quark masses. Clearly the shape of the angular distribution is not very sensitive to the top-quark mass.

Since the Higgs-boson decay to photon pairs is isotropic in the Higgs-boson rest frame, an angular cut of $z < z_0$ retains a fraction z_0 of the decay events. Because the background processes are rather flat out to $z = 0.8$, this is roughly the optimal cut to yield the largest signal-

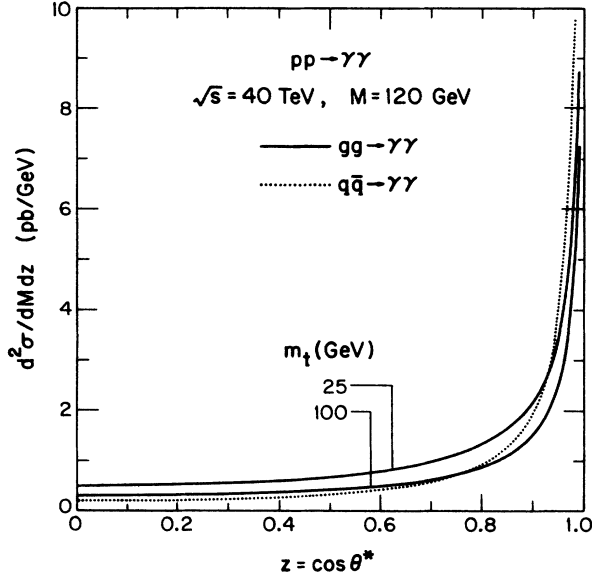


FIG. 5. Angular distribution of photon pairs produced at the SSC via quark-antiquark annihilation and gluon fusion at an invariant mass of 120 GeV. The scattering angle θ^* is in the photon pair center-of-mass system. Duke-Owens set 1 distribution functions were used in the calculation.

to-background ratio while maintaining a maximal number of events. Thus the cut we imposed earlier, following Ref. 7, of $z < 0.5$ is probably too conservative. However, this does not effect the conclusions of Ref. 7 qualitatively.

V. RAPIDITY DISTRIBUTION

Since our goal is to separate the two-photon decay mode of the Higgs boson from the quark-antiquark annihilation and gluon-fusion continuum processes, we are led to investigate differential cross sections with the hope of finding a qualitative difference between the signal and the background. In the previous section we considered the angular distribution of the photons in the photon pair center-of-mass frame. In this section we investigate the rapidity distribution, i.e., the differential probability that the photon pair center-of-mass frame is boosted with respect to the laboratory frame.

The shape of the rapidity distribution (at fixed invariant mass M) depends only on the parton distribution functions. It is given by

$$\frac{d^2\sigma}{dM dy} = \frac{2M}{s} \hat{\sigma} \sum_{i,j} f_i \left[\frac{M}{\sqrt{s}} e^y \right] f_j \left[\frac{M}{\sqrt{s}} e^{-y} \right], \quad (11)$$

where s is the square of the hadronic energy, $\hat{\sigma}$ is the subprocess cross section evaluated at $\hat{s} = M^2$, and $f_i(x)$ is the relevant parton distribution function; the sum runs over the contributing combinations. Since the quark-antiquark annihilation and gluon-fusion processes are initiated by different partons, we expect their rapidity distributions to be different.

In Fig. 6 we give the rapidity distribution of the photon pair center-of-mass frame with respect to the labora-

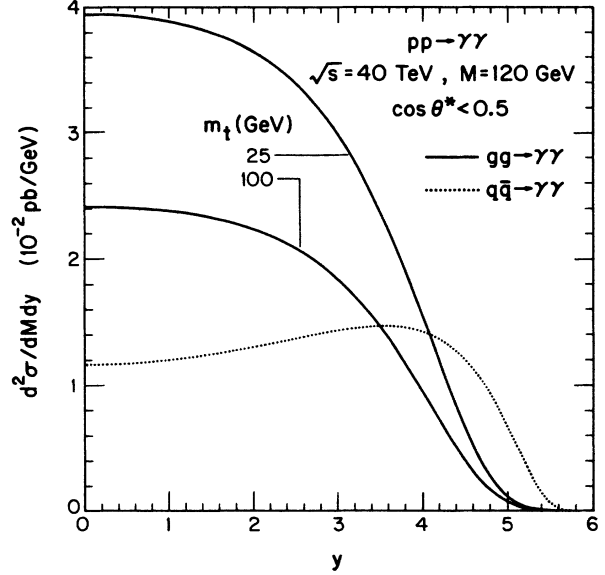


FIG. 6. Rapidity distribution of photon pairs produced at the SSC via quark-antiquark annihilation and gluon fusion at an invariant mass of 120 GeV. Only the positive rapidity region is displayed; the distribution is symmetric about $y = 0$. There is a cut on the scattering angle in the photon pair center-of-mass system θ^* of $\cos\theta^* < 0.5$. Duke-Owens set 1 distribution functions were used in the calculation.

tory frame for photon pairs produced via quark-antiquark annihilation and gluon fusion at the SSC, the latter for two choices of the top-quark mass. Since the distribution is symmetric about $y = 0$, we show only the positive-rapidity half. The photon pair invariant mass is 120 GeV, and we have continued to make an angular cut of $\cos\theta^* < 0.5$. Since the shape of the rapidity distribution depends only on the parton distribution functions, the two gluon-fusion curves differ only by an overall factor.

As we can see from Fig. 6, the gluon-fusion process is peaked at small rapidity, while quark-antiquark annihilation is more evenly distributed over the rapidity range. The gluon distribution function falls off rapidly with x (roughly like $x^{-3/2}$ at the relevant values of x), and hence the gluon luminosity is peaked at small rapidity. The quark-antiquark luminosity is a combination of sea-quark collisions, which favor small rapidity, and sea-quark-valence-quark collisions, which tend to larger rapidities due to the valence-quark distribution functions, which are big at large x .

Since the Higgs boson is produced via gluon fusion, it has the same rapidity distribution as the photon-pair gluon-fusion process. Therefore, a rapidity cut cannot improve the signal-to-background ratio for this background process. However, it can improve the signal-to-background ratio for the quark-antiquark annihilation process. Looking at Fig. 6, we see that a cut near $y = 3$ would optimize the signal-to-background ratio while maintaining a maximal number of events. Therefore the

analysis of Ref. 7 could be slightly improved upon by such a cut, although the qualitative conclusions of that paper remain valid.

VI. LARGE INVARIANT MASSES

Our interest in photon pair production at future hadron colliders stems from our concern with detecting the intermediate-mass Higgs boson in its two-photon decay mode. We have therefore concentrated on photon pair invariant masses between 50 and 200 GeV. However, there may be other processes for which knowledge of the two-photon background at higher invariant masses is important. We therefore present these cross sections for completeness.

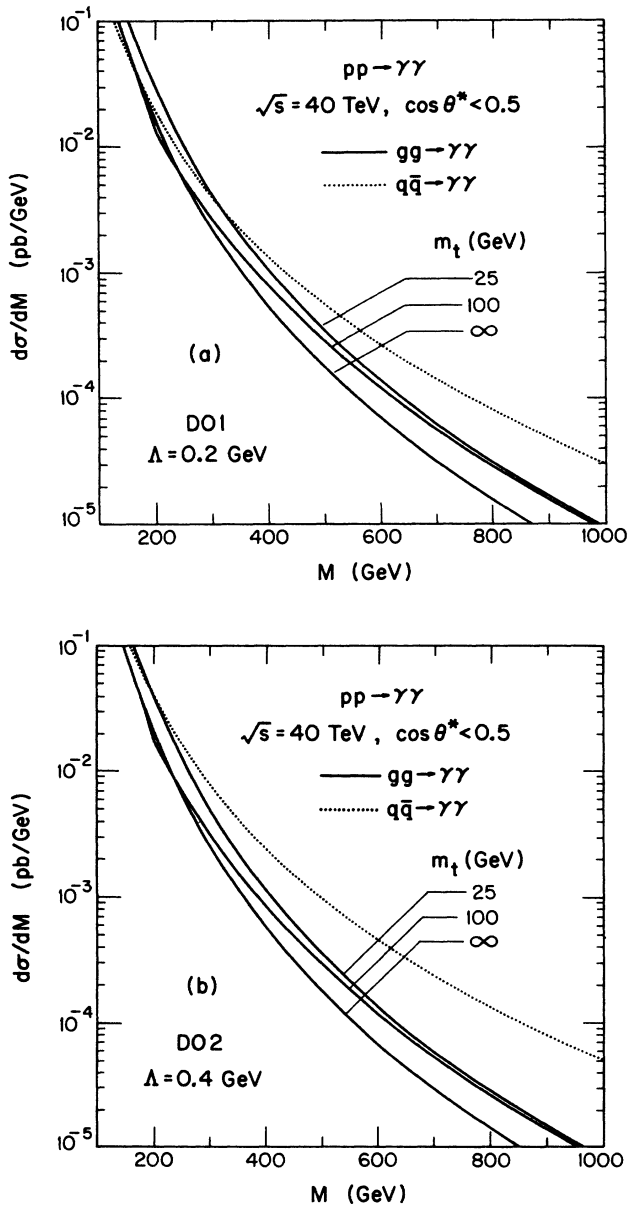


FIG. 7. Invariant-mass distribution of photon pairs as in Fig. 2, but for larger invariant masses.

We display the cross section for photon pair production from gluon fusion and quark-antiquark annihilation at large invariant masses in Figs. 7 (SSC) and 8 (LHC). Since we have continued to use the cut $\cos\theta^* < 0.5$, these figures are extensions of Figs. 2 and 3. Note that the gluon-fusion mechanism is less important than quark-antiquark annihilation as a source of photon pairs as we go to larger invariant masses. This is due to the gluon luminosity, which falls off more rapidly than that of quarks and antiquarks as we probe larger masses.

We show the gluon-fusion cross section for three different top-quark masses; 25 GeV, 100 GeV, and infinity, which is equivalent to ignoring the top-quark contribution. The figures clearly show that the difference between including a light top quark (25 GeV) and not including a top quark in the gluon-fusion cross section is roughly a factor of 2, as we discussed in Sec. 2. The $m_t = 100$ GeV curve has the usual dip at $M = 2m_t$, then asymptotically approaches the $m_t = 25$ GeV curve at large invariant masses.

Figures 7(a) and 7(b) show the dependence of the cross sections on the distribution functions, just as Figs. 2(a) and 2(b) do at smaller invariant masses. We find that the cross sections are less sensitive to the choice of distribution functions at larger invariant masses. For example, at $M = 1$ TeV, the quark-antiquark annihilation cross section increases by a factor of 1.6 for Duke and Owens set 2, compared with a factor of 2 at $M = 200$ GeV.

The gluon-fusion cross section actually decreases for set 2 by a factor of 0.8 at $M = 1$ TeV. Recall that set 2 has a larger value of Λ , and hence more gluons at small x and high Q^2 . This leaves a dearth of gluons at larger values of x , which corresponds to larger invariant masses. This effect is somewhat compensated for by the increased value of α_s associated with a larger Λ . Thus the gluon-fusion cross section at large invariant masses is rather insensitive to the choice of distribution functions.

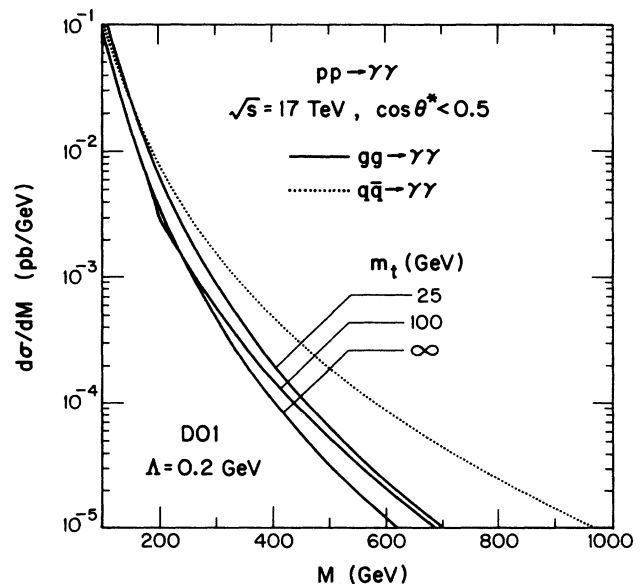


FIG. 8. Invariant-mass distribution of photon pairs as in Fig. 3, but for larger invariant masses.

VII. CONCLUSIONS

We have shown that photon pairs are produced at future hadron colliders just as frequently from gluon fusion [Fig. 1(b)] as from quark-antiquark annihilation [Fig. 1(a)]. The gluon-fusion cross section is sensitive to the mass of the top quark, since each flavor contributes via the loop. We have found that the cross section is roughly twice as large for a light top quark as for a heavy top quark.

Photon pairs are an irreducible background to the two-photon decay mode of the intermediate-mass ($m_H < 2M_W$) Higgs boson. This rare decay mode is only viable if $m_H < 2m_t$, i.e., if the Higgs boson is kinematically forbidden to decay to top quarks. What we have found is that if this inequality is satisfied, then the top-quark contribution to the gluon-fusion continuum background is small. Furthermore, if $m_H \approx 2m_t$, the top-quark contribution interferes destructively with the contribution from the five light quark flavors. This is not a terribly large effect, however; it reduces the cross section by roughly a factor of 0.85. This, in conjunction with the fact that the production cross section is maximized at $m_H \approx 2m_t$, makes this the optimal top-quark mass for hunting the intermediate-mass Higgs boson via its two-photon decay mode.

The signal-to-background ratio for the two-photon decay mode of the Higgs boson has been studied recently in Refs. 5 and 7. In Ref. 5, the gluon-fusion background was calculated neglecting the top-quark contribution; we see that this is justified. In Ref. 7 the gluon-fusion background was approximated by assuming it is roughly equal to the quark-antiquark annihilation background. Since we used the same cuts as Ref. 7, we see that this approxi-

mation is quite good, never off by more than a factor of 2. Therefore, the analyses of Refs. 5 and 7 are reliable, and we refer the reader there for details. Reference 7 concludes that the two-photon decay mode will be viable in the region $100 \text{ GeV} < m_H \lesssim 2M_W$, as long as $m_H < 2m_t$.

We have also found as a result of our study that the signal-to-background ratio can be improved by a judicious choice of cuts, while maintaining a maximal number of events. In particular, we found that a cut on the scattering angle in the photon-pair center-of-mass frame, θ^* , of $\cos\theta^* < 0.8$ ($\theta^* < 37^\circ$) serves to eliminate most of the forward-backward peaking of the quark-antiquark annihilation and gluon-fusion backgrounds. A cut on the rapidity of the photon pair center-of-mass frame with respect to the laboratory frame of roughly $|y| < 3$ (at the SSC) serves to further suppress the quark-antiquark annihilation background.

The implication for detectors is that it is not important to be able to detect photons at small angles or large rapidities. The most important requirement is excellent resolution in the photon pair invariant mass, since the size of the background is directly proportional to the resolution.

ACKNOWLEDGMENTS

We thank J. Gunion and G. Kane for conversations and for providing us with a preliminary version of Ref. 7. We also thank C. Goebel for discussions. This research was supported in part by the University of Wisconsin Research Committee with funds granted by the Wisconsin Alumni Research Foundation, and in part by the U.S. Department of Energy under Contracts Nos. DE-AC02-76ER00881 and DE-FG05-ER8540200.

¹For recent reviews, see the reports in *From Colliders to Super Colliders*, edited by V. Barger and F. Halzen (World Scientific, Singapore, 1987); in *Proceedings of the Summer Study on the Physics of the Superconducting Supercollider*, Snowmass, Colorado, 1986, edited by R. Donaldson and J. Marx (Division of Particles and Fields of the APS, New York, 1987).

²For a recent review, see *Proceedings of the Workshop on Physics at Future Accelerators*, La Thuile, Italy, 1987, edited by J. H. Mulvey (CERN Report No. 87-07, Geneva, 1987).

³E. Eichten, I. Hinchliffe, K. Lane, and C. Quigg, *Rev. Mod. Phys.* **56**, 579 (1984).

⁴I. Hinchliffe, in *Proceedings of the XXIII International Conference on High Energy Physics*, Berkeley, California, 1986, edited by S. Loken (World Scientific, Singapore, 1987), p. 1264.

⁵R. K. Ellis, I. Hinchliffe, M. Soldate, and J. J. van der Bij, *Nucl. Phys.* **B297**, 221 (1988).

⁶J. F. Gunion, P. Kalyniak, M. Soldate, and P. Galison, *Phys. Rev. D* **34**, 101 (1986).

⁷J. F. Gunion, G. L. Kane, and J. Wudka, *Nucl. Phys. B* (to be published).

⁸J. Ellis, M. K. Gaillard, and D. V. Nanopoulos, *Nucl. Phys.* **B106**, 292 (1976); J. P. Leveille, *Phys. Lett.* **83B**, 123 (1979); A. I. Vainshtein, M. B. Voloshin, V. I. Zakharov, and M. A. Shifman, *Yad. Fiz.* **30**, 1368 (1979) [*Sov. J. Nucl. Phys.* **30**,

711 (1979)].

⁹G. Kane, in *Proceedings of the 1986 Summer Study on the Physics of the Superconducting Supercollider* (Ref. 1), p. 7.

¹⁰R. Cahn, M. S. Chanowitz, and N. Fleishon, *Phys. Lett.* **82B**, 113 (1979).

¹¹T. G. Rizzo, *Phys. Rev. D* **22**, 722 (1980); W.-Y. Keung and W. Marciano, *ibid.* **30**, 248 (1984).

¹²L. Ametller, E. Gava, N. Paver, and D. Treleani, *Phys. Rev. D* **32**, 1699 (1985).

¹³B. L. Combridge, *Nucl. Phys.* **B174**, 243 (1980).

¹⁴K. Carimalo, M. Crozon, P. Kessler, and J. Parisi, *Phys. Lett.* **98B**, 105 (1981).

¹⁵E. L. Berger, E. Braaten, and R. D. Field, *Nucl. Phys.* **B239**, 52 (1984).

¹⁶P. Aurenche, R. Baier, A. Douiri, M. Fontannaz, and D. Schiff, *Z. Phys. C* **29**, 459 (1985), A. P. Contogouris, N. Mebarki, and H. Tanaka, *Phys. Rev. D* **35**, 1590 (1987).

¹⁷R. Karplus and M. Neuman, *Phys. Rev.* **83**, 776 (1951).

¹⁸B. De Tollis, *Nuovo Cimento* **32**, 753 (1964); **35**, 1182 (1965).

¹⁹V. Constantini, B. De Tollis, and G. Pistoni, *Nuovo Cimento* **2A**, 733 (1971).

²⁰K. Mitchell, *Philos. Mag.* **40**, 351 (1949); L. Lewin, *Polylogarithms and Associated Functions* (North-Holland, New York, 1981).

²¹G. 't Hooft and M. Veltman, *Nucl. Phys.* **B153**, 365 (1979).

²²G. Passarino and M. Veltman, Nucl. Phys. **B160**, 151 (1979).

²³Although our numerical results, calculated from the analytic amplitudes given in Ref. 19, agree with the numerical results from FORMFACTOR, they do not agree with the numerical results shown in the figures of Ref. 12 (using the cuts in that paper). The numerical values of Ref. 12 seem too large by roughly a factor of 2, although the factor varies with the photon pair invariant mass. Reference 12 also gives numerical results for photon pair production from quark-antiquark annihilation in $p\bar{p}$ collisions; we also disagree with these values by roughly the same amount.

²⁴T. Appelquist and J. Carrazone, Phys. Rev. D **11**, 2856 (1975).

²⁵D. W. Duke and J. F. Owens, Phys. Rev. D **30**, 49 (1984).

²⁶It is proper to include this factor of $\frac{1}{2}$ with the square of the coupling, since the effective strong coupling constant is $\alpha_s/2$.

See the discussion in Sec. 2.15 of F. Halzen and A. D. Martin, *Quarks and Leptons* (Wiley, New York, 1984).

²⁷The enhancement of the box diagram over naive expectations was also noticed by R. N. Cahn and J. F. Gunion, Phys. Rev. D **20**, 2253 (1979).

²⁸This is due to the fact that $\int d^4k/(2\pi)^4 = 1/(8\pi^2) \int k^3 dk$ upon performing the angular integration. This factor, combined with the square of the coupling, leads to the expansion parameter $\alpha/2\pi$, which is the typical size of one-loop effects in QED.

²⁹H. M. Georgi, S. L. Glashow, M. E. Machacek, and D. V. Nanopoulos, Phys. Rev. Lett. **40**, 692 (1978).

³⁰K. J. F. Gaemers and F. Hoogeveen, Phys. Lett. **146B**, 347 (1984).